

## Effect of Molecular Structure on Thermoresponse Behaviors of Pyrrolidone-Based Water-Soluble Polymers

Jun Sun, Yifeng Peng, Ying Chen, Yu Liu, Junjie Deng, Lican Lu, and Yuanli Cai\*

Key Laboratory of Environmentally Friendly Chemistry and Applications of Ministry of Education, Key Laboratory of Advanced Functional Polymeric Materials of College of Hunan Province, Key Laboratory of Polymeric Materials & Application Technology of Hunan Province, College of Chemistry, Xiangtan University, Xiangtan, Hunan 411105, China

Received January 19, 2010; Revised Manuscript Received March 20, 2010

**ABSTRACT:** This paper describes the molecular structure dependent thermoresponse behaviors of pyrrolidone-based water-soluble polymers. A series of well-defined poly[*N*-(2-methacryloyloxyethyl)pyrrolidone] (PNMEP), poly[*N*-(3-acryloyloxypropyl)pyrrolidone] (PNAPP), and poly[*N*-(3-methacryloyloxypropyl)pyrrolidone] (PNMPP) were synthesized via visible light activating RAFT polymerization at 25 °C. Kinetic studies indicate a rapid and well-controlled behavior of this polymerization. Gel permeation chromatography (GPC) and <sup>1</sup>H NMR analysis confirm their intact molecular structure, well-defined molecular weight, and narrow distribution. Laser light scattering and temperature-variable <sup>1</sup>H NMR analyses demonstrate that the cloud point of a PNMEP sample at a degree of polymerization (DP) of 96 is 1.5 °C lower than that of PNAPP at a DP = 104. Additional backbone methyl groups in PNMPP lead to a dramatic cloud point lowering, e.g., cloud point of PNMPP at a DP = 100 is 37 °C lower than that of PNAPP at a DP = 104. This is contrary to what was observed in poly(*N*-isopropylacrylamide) (PNIPA) and its polymethacrylamide analogues. These pyrrolidone-based polymers show a dramatic solvent isotopic effect that is different from that of PNIPA; e.g., the cloud point of PNMEP at a DP = 237 is 8.5 °C lower in D<sub>2</sub>O than in H<sub>2</sub>O. Increasing polymer chain length or hydrophobicity may suppress this solvent isotopic effect. This phase transition is correlated to Hofmeister series but more sensitive than PNIPA. Na<sub>2</sub>CO<sub>3</sub> dramatically lowers cloud point, while NaI significantly improves cloud point, up to full dissolution in H<sub>2</sub>O at 95 °C. The solvent isotopic effect in NaCl or Na<sub>2</sub>CO<sub>3</sub> solution is the same as what observed in solution absent of salt. Upon heating D<sub>2</sub>O solution of PNMEP, the polymer first forms the hydrated irregular colloidal aggregates near the cloud point, the phase transition occurs at the fully hydrated state at cloud point, and further heating leads to the dehydration and separation from D<sub>2</sub>O. However, in NaCl solution, the dehydration of PNMEP occurs subsequently from apolar backbones, spacers, and finally pyrrolidone groups.

### Introduction

Some water-soluble polymers may phase-separate from aqueous solution on heating. The critical temperature of this phase transition is the so-called lower critical solution temperature (LCST). These polymers received increasing attention<sup>1</sup> because of their extensive bio-related applications for protein absorption,<sup>2</sup> controlling bacterial aggregation,<sup>3</sup> drug carriers,<sup>4,5</sup> etc. Thermoresponse behaviors of these polymers depend on their molecular structures. The structural tailorability of monomer units may endow a variety of water-soluble polymers with different thermoresponse behaviors. For example, the gels of poly(*N*-isopropylacrylamide) (PNIPA), poly[*N*-(*n*-propyl)acrylamide], or poly(*N*-cyclopropylacrylamide) have different LCST;<sup>6</sup> poly(*N*-acryloyl-*N'*-propylpiperazine) has a LCST at 37 °C, but its *N'*-methyl or *N'*-ethyl analogues are completely water-soluble;<sup>7,8</sup> poly(*N*-vinylcaprolactam) has a LCST at 31 °C,<sup>9–11</sup> but poly(*N*-vinylpyrrolidone) is completely water-soluble. This temperature-induced phase transition may be adjusted by the polymer backbones; e.g., PNIPA has a lower LCST than poly(*N*-isopropylmethacrylamide) (PNIPMA).<sup>12</sup> The LCST of PNIPA is lower than that of poly(*N,N*-ethylmethacrylamide) because of the formation of PNIPA intra- or interchain hydrogen bonding.<sup>13</sup>

Another noteworthy example is the random copolymers of 2-(2-methoxyethoxy)ethyl methacrylate and oligo(ethylene glycol) methacrylate as described by Lutz and co-workers,<sup>14–16</sup> which cannot form the inter- or intrachain hydrogen bonding. They demonstrate that the temperature-induced phase transition of these polymers is reversible and relatively insensitive to some important parameters such as polymer chain length and concentration and ionic strength of solutions. Moreover, because of this molecular structure character, their aggregates could redissolve readily upon cooling without any noticeable hysteresis.<sup>16</sup> These polymers are very promising for biomedical applications because of their biocompatible oligo(ethylene glycol) segments.

As another possible alternative, pyrrolidone-based polymers may be applied in biomedical fields. Pyrrolidone functionalities endow polymers with some desirable properties, e.g., water solubility, coordination capacity,<sup>17–19</sup> and biocompatibility.<sup>20</sup> As a typical representative, poly(*N*-vinylpyrrolidone) was extensively utilized for dispersing nanoparticles in aqueous solution,<sup>21–24</sup> hemocompatible surface modification,<sup>25</sup> controlled drug delivery,<sup>26,27</sup> bioconjugation, and surface ligand immobilization.<sup>28</sup> Considering these excellent properties and extensive potential applications, the exploitation of thermoresponse behaviors of pyrrolidone-based polymers is clearly far from enough.<sup>29–32</sup>

Early in 1998, Davis and co-workers<sup>30</sup> described the synthesis of pyrrolidone-based polymers via conventional radical

\*Corresponding author: Ph +86-731-58298876; Fax +86-731-58292251; e-mail ylcai98@xtu.edu.cn.

polymerization. They demonstrated that poly[*N*-(2-methacryloyloxyethyl)pyrrolidone] (PNMEP) had a LCST at 29–33 °C, while poly[*N*-(3-methacryloyloxypropyl)pyrrolidone] (PNMPP) could not dissolve in water at room temperature. Clearly, these samples are ill-defined under the conventional radical polymerization. Generally, the LCST of a thermoresponsive polymer depends on its molecular weight and distribution. Polymer samples with intact structure, well-defined molecular weight, and narrow distribution are essential for precise evaluation of their thermoresponsive behaviors.

The reversible addition–fragmentation chain transfer radical polymerization or RAFT polymerization<sup>33</sup> is a powerful tool extensively utilized for the synthesis of well-defined stimuli-responsive polymers.<sup>34–44</sup> Recently, our group developed a rapid and well-controlled visible light activating ambient temperature RAFT polymerization.<sup>45–49</sup> This approach was utilized for the synthesis of well-defined PNMEP samples.<sup>50</sup> Our results demonstrated that PNMEP had a cloud point covering 71.5–52.8 °C at a  $M_w = 20.6\text{--}105.4 \text{ kg mol}^{-1}$ , which is remarkably higher than what observed by Davis and co-workers.<sup>30</sup> Clearly, many aspects including structure dependence, solvent isotopic effect, and salt effect still have to be studied for understanding the thermoresponsive behaviors of these pyrrolidone-based polymers.

This paper describes the structure-dependent thermoresponsive behaviors of pyrrolidone-based polymers. For this purpose, we synthesized a series of well-defined PNMEP and its analogues, i.e., poly[*N*-(3-acryloyloxypropyl)pyrrolidone] (PNAPP) and poly[*N*-(3-methacryloyloxypropyl)pyrrolidone] (PNMPP), via the visible light activating RAFT polymerization at 25 °C. Their cloud points were measured by laser light scattering analysis. The solvent isotopic effect and salt effect on this temperature-induced phase transition and dehydration were evidenced by temperature-variable <sup>1</sup>H NMR and laser light scattering analysis.

## Experimental Section

**Materials.** *S*-1-Ethyl-*S'*-( $\alpha,\alpha'$ -dimethyl- $\alpha'$ -acetic acid)trithiocarbonate (EDMAT)<sup>51</sup> and 2-cyanoprop-2-yl(4-fluoro)dithiobenzoate (CPFDB)<sup>52</sup> were synthesized according to the literature procedures. *N*-Hydroxyethylpyrrolidone (95%) was purchased from Jianhua Co. Ltd. and distilled under reduced pressure. *N,N*-Dimethylformamide (DMF), triethylamine, and ethyl ether were purchased from Shanghai Reagent Co., dried over metallic sodium, and distilled. Chloroform was washed with distilled water, dried over anhydrous calcium chloride overnight, and distilled. (2,4,6-Trimethylbenzoyl)diphenylphosphine oxide (TPO, 97%) was purchased from Runtec Chem. Co.; 3-amino-1-propanol and  $\gamma$ -butyrolactone were purchased from J&K; sodium chloride (NaCl, >99.95%), sodium iodide (NaI, >99.95%), and sodium carbonate (Na<sub>2</sub>CO<sub>3</sub>, >99.95%) were purchased from Shanghai Reagent Co.; methacrylic chloride and acrylic chloride were purchased from Aldrich; heavy water (D<sub>2</sub>O) was purchased from Cambridge Isotope Laboratories Inc.; these reagents were used as received. Highly pure deionized water (H<sub>2</sub>O) at resistivity over 18 M $\Omega$  cm<sup>-1</sup> was utilized. JB400 filters were purchased from Yaguang Sci. Edu. Equip. Co.

**Visible Light Source.** A mercury vapor lamp, emitting separately at 254, 302, 313, 365, 405, 436, 545, and 577 nm, was employed. JB400 filters were utilized to cut off the shorter wave UV light below 400 nm and adjust the light intensity. Thus, a mild visible light, emitting at 405, 436, 545, and 577 nm, at a mild intensity of 250  $\mu\text{W cm}^{-2}$  at 420 nm, was achieved for activating the ambient temperature RAFT polymerization. Light intensity was measured using a UV-A radiometer equipped with a 420 nm sensor.

**Synthesis of *N*-(3-Hydroxypropyl)pyrrolidone.** 3-Amino-1-propanol (41.3 g, 0.55 mol) and  $\gamma$ -butyrolactone (43.0 g, 0.50 mol) were charged in a 100 mL Teflon-lined autoclave. The solution was heated at 230 °C for 10 h. The mixture was distilled under vacuum

to give a transparent product. Weight: 57.6 g; yield: 80.6%. <sup>1</sup>H NMR ( $\delta$ , in CDCl<sub>3</sub>): 3.67 ppm (1H, CH<sub>2</sub>CH<sub>2</sub>CH<sub>2</sub>OH), 3.53 ppm (2H, CH<sub>2</sub>CH<sub>2</sub>CH<sub>2</sub>OH), 3.40 ppm (4H, NCOCH<sub>2</sub>CH<sub>2</sub>CH<sub>2</sub> in pyrrolidone and CH<sub>2</sub>CH<sub>2</sub>CH<sub>2</sub>OH), 2.42 ppm (2H, NCOCH<sub>2</sub>CH<sub>2</sub>CH<sub>2</sub> in pyrrolidone), 2.05 ppm (2H, NCOCH<sub>2</sub>CH<sub>2</sub>CH<sub>2</sub> in pyrrolidone), and 1.69 ppm (2H, CH<sub>2</sub>CH<sub>2</sub>CH<sub>2</sub>OH).

**Synthesis of *N*-(3-Acryloyloxypropyl)pyrrolidone (NAPP) Monomer.** *N*-(3-Hydroxypropyl)pyrrolidone (35.75 g, 0.25 mol), triethylamine (30.30 g, 0.30 mol), and 60.0 mL of anhydrous chloroform were charged in a 500 mL dried round-bottom flask. The flask was immersed in a thermostatic ice bath at 0 °C. Acryloyl chloride (24.89 g, 0.275 mol) solution in 90.0 mL of anhydrous chloroform was added dropwise in this flask for 2 h. The mixture was stirred at 10 °C for 12 h. The white ammonium salt was removed by filtration. The solution was concentrated by rotary evaporation. The solution was extracted using subsequently a 5% Na<sub>2</sub>CO<sub>3</sub> solution, a saturated NaCl solution, and distilled water until neutralization. The solution was dried over anhydrous MgSO<sub>4</sub> and distilled under vacuum to give a transparent targeted monomer. Weight: 34.3 g; yield: 69%. <sup>1</sup>H NMR ( $\delta$ , in D<sub>2</sub>O): 6.25, 6.06, and 5.83 ppm (3H, CH<sub>2</sub>=CH), 4.04 ppm (2H, COOCH<sub>2</sub>CH<sub>2</sub>CH<sub>2</sub>), 3.22–3.34 ppm (4H, NCOCH<sub>2</sub>CH<sub>2</sub>CH<sub>2</sub> in pyrrolidone and COOCH<sub>2</sub>CH<sub>2</sub>CH<sub>2</sub>), 2.26 ppm (2H, NCOCH<sub>2</sub>CH<sub>2</sub>CH<sub>2</sub> in pyrrolidone), 1.81–1.87 ppm (4H, NCOCH<sub>2</sub>CH<sub>2</sub>CH<sub>2</sub> in pyrrolidone and COOCH<sub>2</sub>CH<sub>2</sub>CH<sub>2</sub>).

The procedure for the synthesis of *N*-(3-methacryloyloxypropyl)pyrrolidone (NMPP) was the same as above, except for using methacrylic chloride. <sup>1</sup>H NMR ( $\delta$ , in D<sub>2</sub>O): 6.08 and 5.67 ppm (2H, CH<sub>2</sub>=CCH<sub>3</sub>), 4.14 ppm (2H, COOCH<sub>2</sub>CH<sub>2</sub>CH<sub>2</sub>), 3.35–3.47 ppm (4H, NCOCH<sub>2</sub>CH<sub>2</sub>CH<sub>2</sub> in pyrrolidone and COOCH<sub>2</sub>CH<sub>2</sub>CH<sub>2</sub>), 2.37 ppm (2H, NCOCH<sub>2</sub>CH<sub>2</sub>CH<sub>2</sub> in pyrrolidone), 1.88–2.00 ppm (7H, COOCH<sub>2</sub>CH<sub>2</sub>CH<sub>2</sub>, CH<sub>2</sub>=CCH<sub>3</sub>, NCOCH<sub>2</sub>CH<sub>2</sub>CH<sub>2</sub> in pyrrolidone). *N*-(2-Methacryloyloxyethyl)pyrrolidone (NMEP) monomer was synthesized according to our previous paper.<sup>50</sup>

**Visible Light Activating RAFT Polymerization of NAPP at 25 °C.** NAPP (5.91 g, 30.0 mmol), EDMAT (25.2 mg, 0.3 mmol), TPO (5.85 mg, 0.045 mmol), and 3.00 g of anhydrous DMF were charged in a 25 mL round-bottom flask capped with rubber septa. The solution was deoxygenated by purging with highly pure nitrogen gas for 40 min. The solution was irradiated with visible light under stirring at 25 °C. Samples were collected using deoxygenated syringes at predetermined intervals, quenched by exposure to air and addition of traces of hydroquinone inhibitor. One portion of sample was diluted in CDCl<sub>3</sub> for <sup>1</sup>H NMR analysis; another portion was diluted in DMF for GPC measurement. The NAPP monomer conversions were assessed by <sup>1</sup>H NMR according to eq 1:

$$\text{conversion} = \frac{I_{3.88-4.24} - \frac{2}{3}I_{5.75-6.48}}{I_{3.88-4.24}} \times 100\% \quad (1)$$

where  $I_{3.88-4.24}$  is the integral of proton resonance signals at  $\delta = 3.88\text{--}4.24$  ppm (COOCH<sub>2</sub>CH<sub>2</sub>CH<sub>2</sub> of NAPP monomer and PNAPP polymer) and  $I_{5.75-6.48}$  is the integral of proton resonance signals at  $\delta = 5.75\text{--}6.48$  ppm (CH<sub>2</sub>=CH of NAPP monomer).

The procedure for the visible light activating RAFT polymerization of NMEP or NMPP at 25 °C is the same as above, except for using CPFDB chain transfer agent at different feed molar ratios.

**Laser Light Scattering Measurements.** The light scattering intensities were measured by laser light scattering (LLS) on a BI-200SM Brookhaven instrument being equipped with a 100 mW adjustable solid-state laser emitting at 532 nm, a BI-200SM goniometer, and a BI-9000 digital correlator. The laser was adjusted to 43 mW prior to measurements. A BI-TCDC temperature controller was utilized for precisely adjusting the solution temperature. The solutions were heated in steps and stabilized

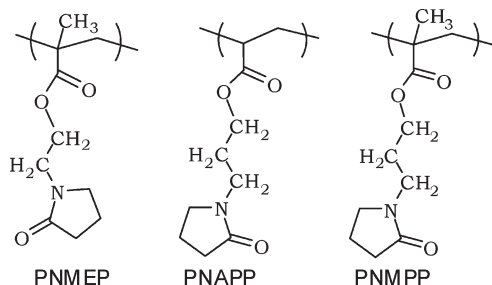


**Figure 1.** Molecular structures of poly[*N*-(2-methacryloyloxyethyl)pyrrolidone] (PNMEP), poly[*N*-(3-acryloyloxypropyl)pyrrolidone] (PNAPP), and poly[*N*-(3-methacryloyloxypropyl)pyrrolidone] (PNMPP).

for 2 min before recording the data. The light scattering intensities at an angle of 90° were recorded.

**GPC measurements** were performed on a PL-GPC120 setup being equipped with a column set consisting of two PL gel 5 μm MIXED-D columns (7.5 × 300 mm, effective molecular weight range of 0.2–400.0 kg mol<sup>-1</sup>), using DMF as an eluent that contained 0.01 M LiBr at 80 °C at a flow rate of 1.0 mL min<sup>-1</sup>. Narrow-distributed polystyrene standards in molecular weight range of 0.5–7500.0 kg mol<sup>-1</sup> (PSS, Mainz, Germany) were utilized for calibration.

**<sup>1</sup>H NMR analysis** was performed on a 400 MHz Bruker AV-400 NMR spectrometer equipped with a temperature controller. Except for the temperature-variable <sup>1</sup>H NMR measurements, other samples were measured at 20 °C.

## Results and Discussion

Davis and co-workers<sup>30</sup> and our group<sup>50</sup> demonstrated that PNMEP had a LCST behavior. The pendant pyrrolidone groups provide the water solubility via hydrogen bonding with the adjacent water molecules. Indeed, this hydrogen bonding is the key factor for the excellent water solubility of poly(*N*-vinylpyrrolidone). On the other hand, the hydrophobicity of apolar backbones and spacers of PNMEP counterbalances this dissolving-favorable effect. Unlike the temperature-induced phase transition of widely studied PNIPAA, PNMEP cannot form the inter- or intrachain hydrogen bonding. Thus, its temperature-induced aggregates could readily redissolve upon cooling, without any noticeable hysteresis.<sup>50</sup> This phenomenon was also observed in the aqueous solution of random copolymer of 2-(2-methoxyethoxy)ethyl methacrylate and oligo(ethylene glycol) methacrylate.<sup>16</sup>

In order to further elucidate the thermoresponsive behaviors of polymers with this structure character, we synthesized a series of PNMEP and its two analogues, i.e., poly[*N*-(3-acryloyloxypropyl)pyrrolidone] (PNAPP) and poly[*N*-(3-methacryloyloxypropyl)pyrrolidone] (PNMPP), via the visible light activating RAFT polymerization at 25 °C.<sup>45–49</sup> As shown in Figure 1, the elemental composition of PNAPP is the same as that of PNMEP, but their backbones and spacers are different; PNMPP and PNMEP have the same methacrylic backbones, but PNMPP has one more methylene in spacers.

NAPP and NMPP monomers were synthesized via esterifying *N*-(3-hydroxypropyl)pyrrolidone separately with acryloyl chloride and methacryloyl chloride. As shown in Figure 2a, the integral ratio of proton signals  $I_a:I_b:I_{a'}:I_c:I_{e+f}:I_h:I_{d+g}$  equals 1:1:1:2:4:2:4. Moreover, except for the proton signal of HOD, no other signal of impurities is detectable. These suggest the high purity of NAPP monomer. <sup>1</sup>H NMR analysis also confirms the high purity of NMPP monomer (see Figure 2b).

**Synthesis of Poly[*N*-(3-acryloyloxypropyl)pyrrolidone] (PNAPP).** This polymer was synthesized via the visible light activating RAFT polymerization of NAPP monomer at

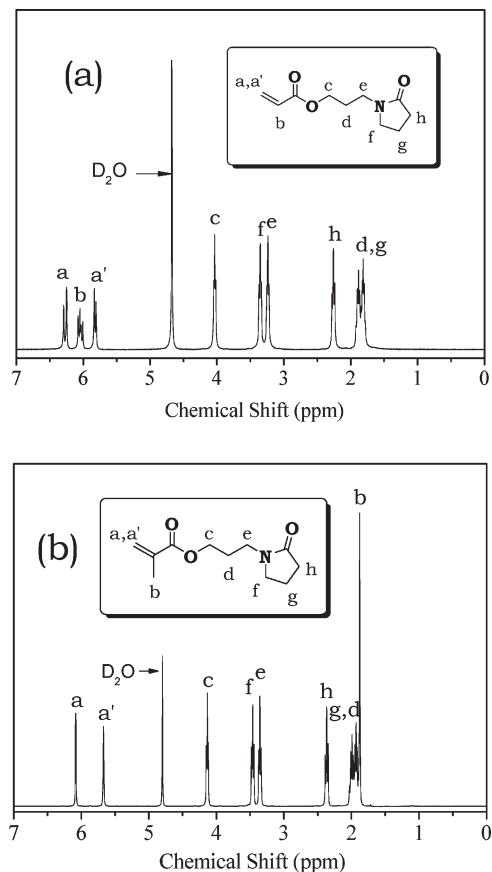


**Figure 2.** <sup>1</sup>H NMR spectra of (a) *N*-(3-acryloyloxypropyl)pyrrolidone (NAPP) and (b) *N*-(3-methacryloyloxypropyl)pyrrolidone (NMPP) monomers in D<sub>2</sub>O.

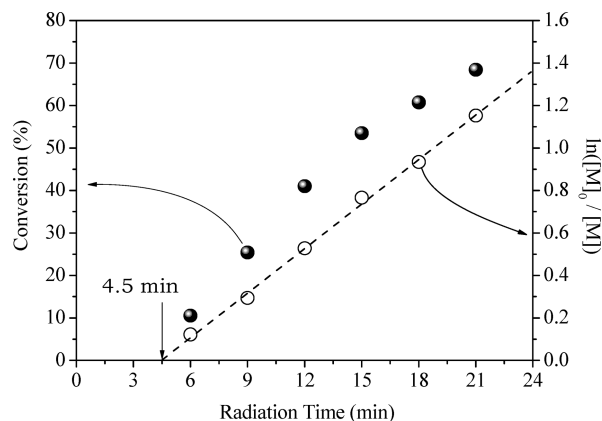


**Figure 3.** Kinetic curves of the visible light activating RAFT polymerization of *N*-(3-acryloyloxypropyl)pyrrolidone (NAPP) using a *S*-1-ethyl-*S'*-( $\alpha,\alpha'$ -dimethyl- $\alpha'$ -acetic acid)trithiocarbonate (EDMAT) chain transfer agent and a (2,4,6-trimethylbenzoyl)diphenylphosphine oxide (TPO) photoinitiator at  $[NAPP]_0:[EDMAT]_0:[TPO]_0 = 200:1:0.15$  in 40 wt % *N,N*-dimethylformamide (DMF) at 25 °C.

25 °C. As shown in Figure 3, at a feed molar ratio of  $[NAPP]_0:[EDMAT]_0:[TPO]_0 = 200:1:0.15$ , this polymerization proceeds rapidly, 68% monomer polymerized in 21 min. The initialization period<sup>53,54</sup> is just 4.5 min. Moreover, the semilogarithmic kinetic curve exhibits a linear evolution on radiation time, suggesting a first-order kinetic character of this RAFT polymerization. This indicates that the radical concentration is constant and steady over the duration of this RAFT polymerization.

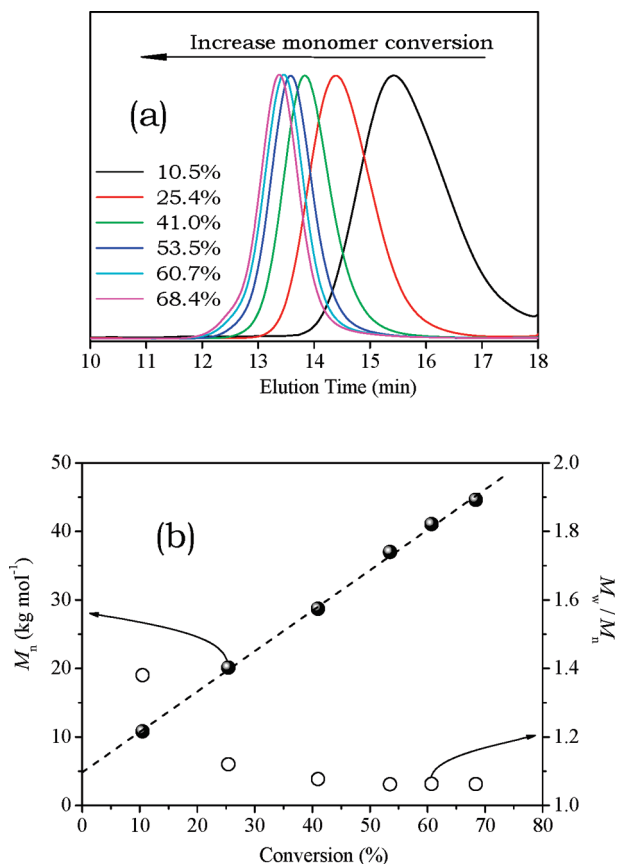


**Figure 4.** (a) GPC trace evolution of poly[*N*-(3-acryloyloxypropyl)pyrrolidone] (PNAPP) synthesized under the same polymerizing conditions as described in Figure 3. (b) Number-average molecular weight ( $M_n$ ) (solid) and polydispersity index ( $M_w/M_n$ ) (hollow) of this polymer as a function of monomer conversions.

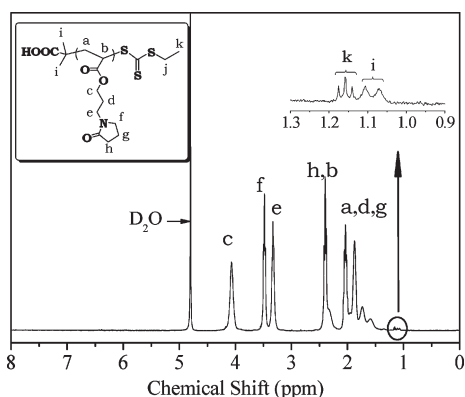


**Figure 5.**  $^1\text{H}$  NMR spectrum of poly[*N*-(3-acryloyloxypropyl)pyrrolidone] (PNAPP, GPC:  $M_n = 40.7 \text{ kg mol}^{-1}$ ,  $M_w/M_n = 1.10$ ) in  $\text{D}_2\text{O}$ .

As shown in Figure 4a, the GPC trace clearly shifts to higher molecular weight side and gradually narrows down on increasing monomer conversion. These GPC traces are monomodal and symmetrical over 50% monomer conversions. As shown in Figure 4b, the number-average molecular weight ( $M_n$ ) of PNAPP linearly increases with monomer conversions. Moreover, the polydispersity index is reasonably narrow at the early stage, e.g.,  $M_w/M_n = 1.12$  at 25% monomer conversion, which lowers down to 1.07 over 40% monomer conversions. This suggests a well-controlled behavior of this RAFT polymerization. Clearly, these molecular weights are overestimated by GPC analysis, most

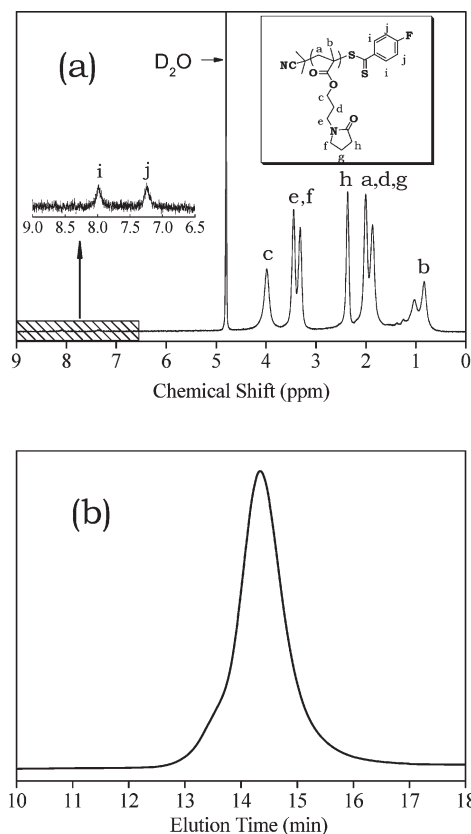


**Figure 6.**  $^1\text{H}$  NMR spectrum (a) and GPC trace (b) of poly[*N*-(3-methylacryloyloxypropyl)pyrrolidone] (PNMPP).

presumably due to the calibration errors caused by using polystyrene standards. Thus, the number-average molecular weights of these polymers based on  $^1\text{H}$  NMR analysis were utilized for evaluating the thermoresponsive behavior.

As shown in Figure 5, no signal at  $\delta = 5.5\text{--}6.5$  ppm ( $\text{CH}_2=\text{CH}$  of NAPP monomer) is detectable, which indicates that NAPP monomer was completely removed from the final PNAPP sample. The integral ratio of  $I_c:I_e:I_{h+b}:I_{a+d+j} = 2:2:2:3:6$  within the analysis errors. This suggests the intact structure of this targeted polymer. Except for the proton signal of HOD, no proton signal of other impurities is detectable, indicating the high purity of this polymer sample. Moreover, as shown in the inset of Figure 5, the proton signals at  $\delta = 1.0\text{--}1.2$  ppm ( $\text{SCH}_2\text{CH}_3$  and  $\text{C}(\text{CH}_3)_2\text{COOH}$  of EDMAT residues at the chain ends) are detectable; thus,  $M_n$  may be assessed according to eq 2:

$$M_n = \frac{4.5I_c}{I_{i+k}}M_{\text{NAPP}} + M_{\text{EDMAT}} \quad (2)$$

where  $M_{\text{NAPP}}$  and  $M_{\text{EDMAT}}$  are the molecular weights of NAPP monomer and EDMAT chain transfer agent.  $^1\text{H}$  NMR analysis gives a  $M_n$  of  $20.7 \text{ kg mol}^{-1}$ ; thus, the polymer chain length is denoted by the degree of polymerization (DP) of 104.

**Synthesis of Poly(*N*-(3-methacryloyloxypropyl)pyrrolidone) (PNMPP).** As shown in Figure 6a, no signal at  $\delta = 5.5\text{--}6.5$  ppm ( $\text{CH}_2=\text{CCH}_3$  of NMPP monomer) is detectable, indicating that NMPP monomer was completely removed from this final PNMPP sample. The integral ratio of  $I_c:I_{e+f}:I_{h+a+d+g}:I_b = 2:4:2:6:3$ . This suggests the intact structure of this PNMPP sample. Except for the proton signal of HOD, no proton signal of other impurities is detectable, indicating the

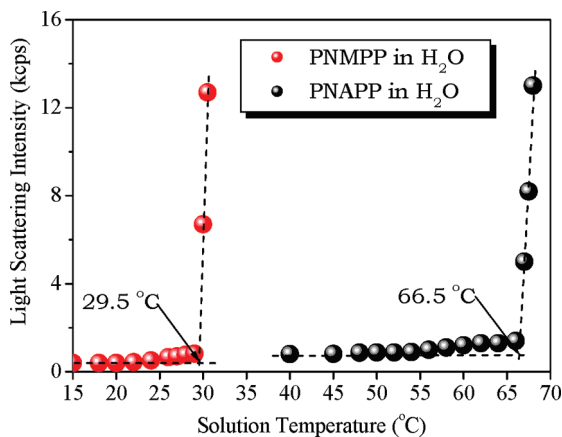


**Figure 7.** Light scattering intensity of a 20.0 mg mL<sup>-1</sup> poly[*N*-(3-acryloyloxypropyl)pyrrolidone] (PNAPP, <sup>1</sup>H NMR:  $M_n = 20.7$  kg mol<sup>-1</sup>; GPC:  $M_n = 40.7$  kg mol<sup>-1</sup>,  $M_w/M_n = 1.10$ ) or poly[*N*-(3-methylacryloyloxypropyl)pyrrolidone] (PNMPP, <sup>1</sup>H NMR:  $M_n = 21.3$  kg mol<sup>-1</sup>; GPC:  $M_n = 24.4$  kg mol<sup>-1</sup>,  $M_w/M_n = 1.10$ ) aqueous solution as a function of solution temperature.

high purity of this polymer sample. As shown in the inset of Figure 6, the proton signals at  $\delta = 7.0$ – $8.5$  ppm (4H in 4-fluorobenzene of CPFDB residues at the polymer chain ends) are detectable; thus,  $M_n$  may be assessed according to eq 3:

$$M_n = \frac{2I_c}{I_{i+j}} M_{\text{NMPP}} + M_{\text{CPFDB}} \quad (3)$$

where  $M_{\text{NMPP}}$  and  $M_{\text{CPFDB}}$  are the molecular weights of NMPP monomer and CPFDB chain transfer agent. <sup>1</sup>H NMR analysis gives a  $M_n$  of 21.3 kg mol<sup>-1</sup>, or DP = 100, which is comparable to that of its corresponding PNAPP analogue as mentioned above. Moreover, as shown in Figure 6b, the GPC trace of this polymer is reasonably symmetrical and gives a narrow distribution of  $M_w/M_n = 1.10$ .

**Effect of Molecular Structure on Temperature-Induced Phase Transition.** As shown in Figure 7, PNMPP was fully dissolved in water at solution temperature below 25 °C. On heating up to 29.5 °C, the light intensity dramatically increased, suggesting the occurrence of phase transition. This critical temperature was the so-called cloud point. The transparent solution changed to milky, and the polymer settled down at the bottom of vial on further heating to 32 °C and kept for 2 h. However, as described by Iskander et al.,<sup>30</sup> the PNMPP sample synthesized via conventional radical polymerization is water-insoluble at room temperature. This implies that the molecular weight of their PNMPP sample is at least higher than 21.3 kg mol<sup>-1</sup>.

In contrast, at a DP = 104, PNAPP exhibits a cloud point of 66.5 °C, which is 37 °C higher than that of the above-mentioned PNMPP (DP = 100). This difference is contrary to what was observed in PNIPAA and its poly(*N*-isopropylmethacrylamide) (PNIPMA) analogue; the LCST of PNIPAA is 13 °C lower than that of PNIPMA due to the restrained intrachain collapse and interchain association by the additional backbone methyl groups in PNIPMA.<sup>12</sup> Unlike PNIPAA or PNIPMA, PNAPP or PNMPP cannot form the intra- or interchain hydrogen bonding; thus, the temperature-induced phase transition attributes to the enhanced effect of hydrophobic association.

As shown in Figure 8, over a relatively low molecular weight range of  $M_n = 16.2$ – $19.2$  kg mol<sup>-1</sup>, the cloud point dramatically lowers down on increasing molecular weight. This dramatic decrease attributes to the reduced mixing

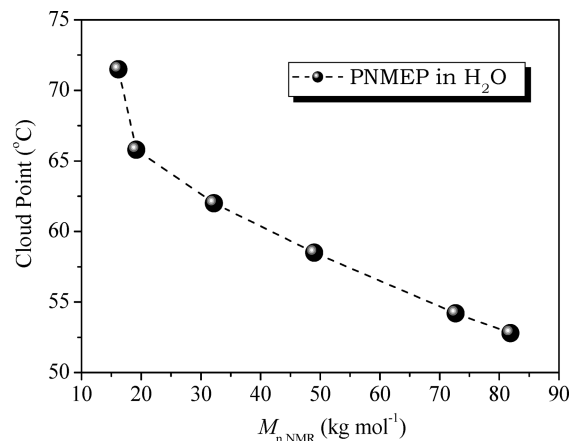


**Figure 8.** Cloud point of poly[*N*-(2-methacryloyloxyethyl)pyrrolidone] (PNMEP) aqueous solution as a function of the number-average molecular weight ( $M_n$ ) of this polymer. All PNMEP samples are narrow-distributed with polydispersity indices of  $M_w/M_n = 1.08$ – $1.13$ , as measured by GPC analysis.

entropy on increasing molecular weight<sup>55,56</sup> because the lowering tendency clearly slows down on further increasing  $M_n$  from 19.2 to 81.9 kg mol<sup>-1</sup>. As derived from Figure 8, at the same  $M_n$  of 20.7 kg mol<sup>-1</sup>, PNMEP shows a cloud point of 65.3 °C, which is 1.2 °C lower than that of its PNAPP analogue. Generally, for PNAPP, the acrylic backbone facilitates the chain conformational adjusting, and the additional spacer methylene enhances the hydrophobic association. This structure effect seems to lower the cloud point. We cannot give a reasonable explanation at present.

**Solvent Isotopic Effect on Thermoresponsive Behaviors.** As shown in Figure 9, in light water (H<sub>2</sub>O), PNMEP at DP = 237 exhibits a cloud point of 58.3 °C. This cloud point linearly lowers down to 49.8 °C in D<sub>2</sub>O on increasing molar fraction of heavy water (D<sub>2</sub>O) (see Supporting Information Figure S1), 8.5 °C lower than in H<sub>2</sub>O. Cremer and co-workers<sup>59</sup> also observed a lowering LCST of elastin-like polypeptides in D<sub>2</sub>O than in H<sub>2</sub>O. However, this lowering tendency is contrary to what was observed in PNIPAA, whose LCST is ~1 °C higher in D<sub>2</sub>O than in H<sub>2</sub>O.<sup>60,61</sup>

In D<sub>2</sub>O solution at 48 °C, ca. 2 °C below the cloud point of 49.8 °C, the light scattering analysis revealed a strong angular dependence of hydrodynamic diameters ( $D_h$ ) of aggregates roughly at 53–238 nm over a measuring angle range of 45°–120°. However, as kept the solution at 48 °C for 2 h, the intensity was essentially constant at 2.5 kcps (see Figure 10), and  $D_h$  at roughly 200–260 nm, as measured at a fixed angle of 90°. These indicate the formation of irregular colloidal aggregates. Based on <sup>1</sup>H NMR analysis, the integral ratio of PNMEP proton signals at 48 °C is essentially the same as that at 20 °C, suggesting the fully hydrated state of these aggregates.

As shown in Figure 10, in D<sub>2</sub>O solution at 52 °C, ca. 2 °C over the cloud point of 49.8 °C, this solution became turbid immediately, and the intensity increased at the beginning; it rapidly lowered down after 15 min. Further keeping this solution at 52 °C for 5 h, the polymer settled down at the bottom of vial as an oily consistency. This suggests the macrophase separation rather than the formation of colloidal aggregates.

On the basis of the results of Cremer and co-workers,<sup>59</sup> hydrogen bonding rather than hydrophobicity is the key factor in the stabilization of the collapsed state of elastin-like polypeptides in D<sub>2</sub>O. However, the hydrogen bonding of PNIPAA amides with the adjacent D<sub>2</sub>O molecules is ~5%

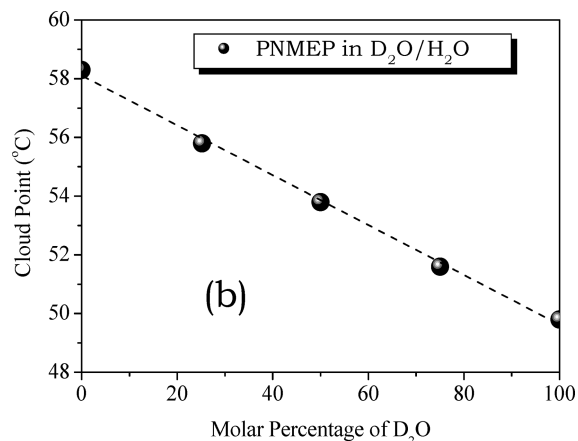


**Figure 9.** Cloud point of a 20.0 mg mL<sup>-1</sup> poly[*N*-(2-methacryloyloxyethyl)pyrrolidone] (PNMEP, <sup>1</sup>H NMR:  $M_n = 47.0$  kg mol<sup>-1</sup>; GPC:  $M_n = 39.0$  kg mol<sup>-1</sup>,  $M_w/M_n = 1.09$ ) in the mixed solvent of D<sub>2</sub>O and H<sub>2</sub>O as a function of molar percentage of D<sub>2</sub>O.

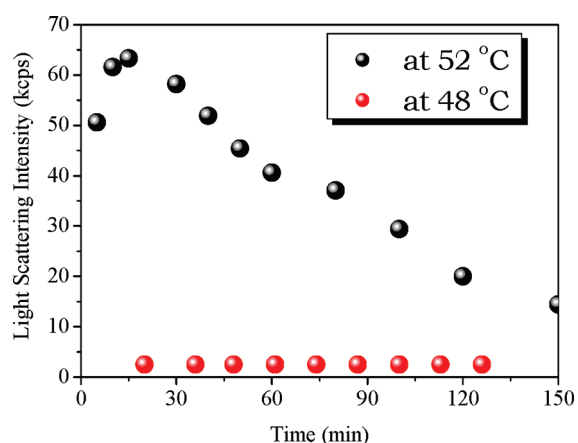


**Figure 10.** Light scattering intensity of a 20.0 mg mL<sup>-1</sup> poly[*N*-(2-methacryloyloxyethyl)pyrrolidone] (PNMEP, <sup>1</sup>H NMR:  $M_n = 47.0$  kg mol<sup>-1</sup>; GPC:  $M_n = 39.0$  kg mol<sup>-1</sup>,  $M_w/M_n = 1.09$ ) solution in D<sub>2</sub>O, separately at 48 or 52 °C, as a function of time for keeping this temperature.

stronger than that with H<sub>2</sub>O molecules;<sup>62</sup> thus, breaking these hydrogen bonds is more enthalpically costly in D<sub>2</sub>O.<sup>63</sup> This leads to a more extended conformation<sup>64</sup> or higher LCST<sup>60</sup> of PNIPA in D<sub>2</sub>O than in H<sub>2</sub>O. Nevertheless, there is no strong hydrogen bond donor in PNMEP but weaker van der Waals interaction, including hydrophobic association of apolar backbones and spacers. Thus, this significant LCST lowering attributes to this structure character. Clearly, further intensive studies are necessary to clarify this phenomenon.

In order to elucidate this solvent isotopic effect, a PNMEP at a long chain length of DP = 415 was utilized for laser light scattering analysis and temperature-variable <sup>1</sup>H NMR measurements. As shown in Figure 11a, its cloud point is 8.0 °C lower in D<sub>2</sub>O than in H<sub>2</sub>O. This  $\Delta T$  is 0.5 °C smaller than that of the above-mentioned shorter one. This suggests that the increase of chain length may suppress this solvent isotopic effect.

The temperature-induced dehydration was quantitatively assessed by temperature-variable <sup>1</sup>H NMR analysis, using the proton signal of HOD in D<sub>2</sub>O solvent as an external standard. Considering the constant concentration of HOD in this solution at 22–60 °C, the temperature-induced dehydration may be detected based on the attenuation of PNMEP protons as compared with the proton signal of HOD.

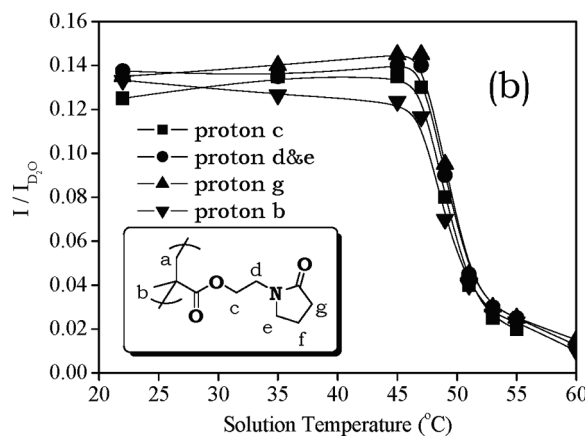
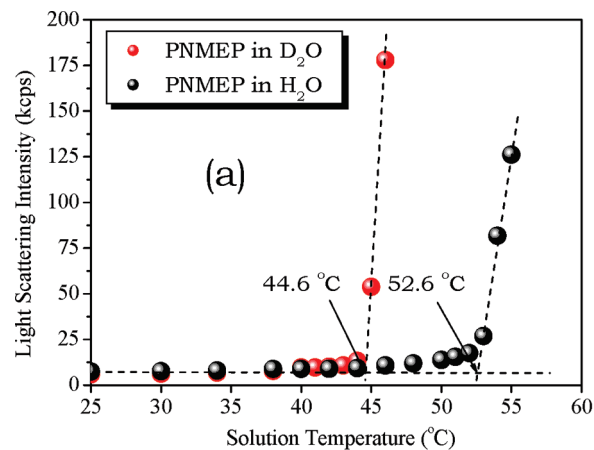


**Figure 11.** (a) Light scattering intensity of a 16 mg mL<sup>-1</sup> poly[*N*-(2-methacryloyloxyethyl)pyrrolidone] (PNMEP, <sup>1</sup>H NMR:  $M_n = 81.9$  kg mol<sup>-1</sup>; GPC:  $M_n = 85.0$  kg mol<sup>-1</sup>,  $M_w/M_n = 1.11$ ) in H<sub>2</sub>O or D<sub>2</sub>O as a function of solution temperature. (b) The integral ratios of each PNMEP proton to that of D<sub>2</sub>O ( $I/I_{D_2O}$ ) as a function of solution temperature.

As shown in Figure 11b, on heating the solution from 22 to 46 °C, the integral ratios of protons in either pyrrolidone rings or COOCH<sub>2</sub>CH<sub>2</sub> keep essentially constant within the analysis errors. This indicates the full hydration of this polymer. The integral ratio relative to the backbone methyl protons was slightly attenuated on elevating solution temperature. These integral ratios dramatically decrease on further heating the solution up to 51.9 °C. Thereafter, this decrease tendency slows down up to 60 °C.

It should be noted that we were previously misled and drew a wrong conclusion, simply based on these temperature-variable <sup>1</sup>H NMR results.<sup>50</sup> Actually, according to the light scattering results as shown in Figure 11a, in D<sub>2</sub>O solution, the cloud point of this polymer is at 44.6 °C, which is 1.4 °C lower than the critical temperature of 46 °C, where the integral ratios dramatically decrease. This suggests that the dehydration temperature is higher than the cloud point, rather than below this cloud point as described in our previous paper.<sup>50</sup>

As shown in Figure 12, the cloud point of PNMP at a DP = 100 is 2.8 °C lower in D<sub>2</sub>O than in H<sub>2</sub>O, much less pronounced than the LCST difference of above-mentioned PNMEP samples. This suggests that the enhanced spacer hydrophobicity suppresses this solvent isotopic effect.

**Salt Effect on Thermoresponsive Behaviors.** Na<sub>2</sub>CO<sub>3</sub> significantly lowers the cloud point of PNMEP from 58.3 °C in deionized H<sub>2</sub>O down to 36.7 °C in 0.101 mol L<sup>-1</sup> Na<sub>2</sub>CO<sub>3</sub>

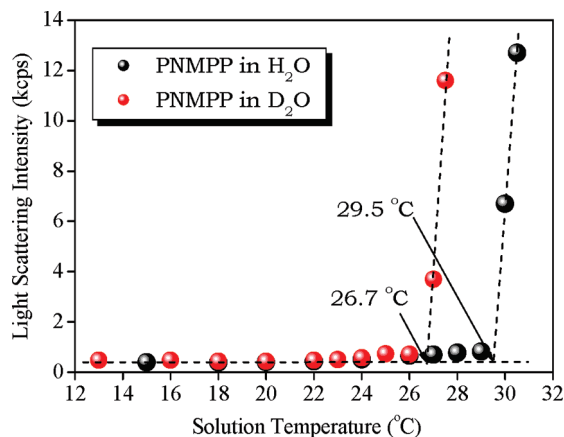


**Figure 12.** Light scattering intensity of a 20 mg mL<sup>-1</sup> poly[*N*-(3-methacryloyloxypropyl)pyrrolidone] (PNMPP, <sup>1</sup>H NMR:  $M_n = 21.3$  kg mol<sup>-1</sup>; GPC:  $M_n = 24.4$  kg mol<sup>-1</sup>,  $M_w/M_n = 1.10$ ) in H<sub>2</sub>O or D<sub>2</sub>O as a function of solution temperature.

aqueous solution (see Supporting Information Figure S2). As derived from Figure 13a, this cloud point linearly lowers down at a slope ( $\Delta T/\Delta C_{\text{Na}_2\text{CO}_3}$ ) of  $-218$  °C/mol L<sup>-1</sup>, which is remarkably more pronounced than what observed in PNIPA ( $-27$  °C/mol L<sup>-1</sup>).<sup>57</sup> This suggests that the addition of Na<sub>2</sub>CO<sub>3</sub> significantly enhances the hydrophobic association. In addition,  $\Delta T/\Delta C_{\text{Na}_2\text{CO}_3}$  in D<sub>2</sub>O is the same as that in H<sub>2</sub>O, suggesting the same solvent isotopic effect, in either the absence or presence of NaCO<sub>3</sub>.

The addition of NaCl also lowers the cloud point from 58.3 °C in deionized H<sub>2</sub>O down to 38.9 °C in 0.999 mol L<sup>-1</sup> NaCl aqueous solution (see Supporting Information Figure S3). As derived from Figure 13b, the cloud point linearly lowers down with NaCl concentration at a slope ( $\Delta T/\Delta C_{\text{NaCl}}$ ) of  $-19$  °C/mol L<sup>-1</sup>, but less pronounced than the above-mentioned  $\Delta T/\Delta C_{\text{Na}_2\text{CO}_3}$ . However, it is somewhat higher than that of PNIPA ( $-10$  °C/mol L<sup>-1</sup>).<sup>58</sup> In addition,  $\Delta T/\Delta C_{\text{NaCl}}$  in D<sub>2</sub>O is the same as that in H<sub>2</sub>O, suggesting the same solvent isotopic effect, in either the absence or presence of NaCl.

However, as shown in Figure 13c, the cloud point significantly improves on the addition of NaI, e.g., from 58.3 °C in deionized H<sub>2</sub>O up to 79 °C in 0.0995 mol L<sup>-1</sup> NaI aqueous solution (see Supporting Information Figure S4). Further increasing the concentration of NaI up to 1.0 mol L<sup>-1</sup> leads to the full dissolution of this polymer up to 95 °C. This phenomenon is different from what observed in PNIPA.<sup>58</sup>

In summary, similar to the widely studied effect of Hofmeister anions on LCST of PNIPA<sup>65,66,57</sup> or elastin-like polypeptides,<sup>59</sup> the phase transition of PNMEP is also correlated to Hofmeister series.<sup>67–70</sup> CO<sub>3</sub><sup>2-</sup> or Cl<sup>-</sup> anions polarize their adjacent water molecules, which are in turn involved in hydrogen bonding with pyrrolidones, thus modulating the hydrophobic hydration, leading to a salting-out effect or lowering the cloud point. However, I<sup>-</sup> anions may bind directly to the amides of pendant pyrrolidone groups,<sup>57</sup> leading to a salting-in effect, up to fully dissolving this polymer at 95 °C.

As shown in Figure 14, the integral ratio of PNMEP proton signals equals the hydrogen ratio of this polymer, suggesting that this polymer was fully dissolved in D<sub>2</sub>O at 20 °C. On the other hand, in NaCl solution, these proton signals shift to low magnetic field. This suggests that NaCl disturbs the chemical environment of polymer protons. This disturbance is more pronounced in NaI solution, leading to the signals shift to much lower magnetic field. The signal of

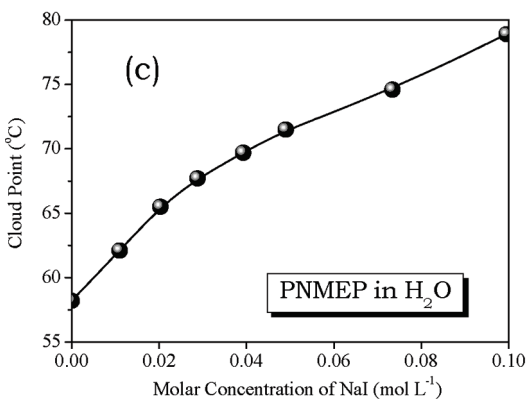
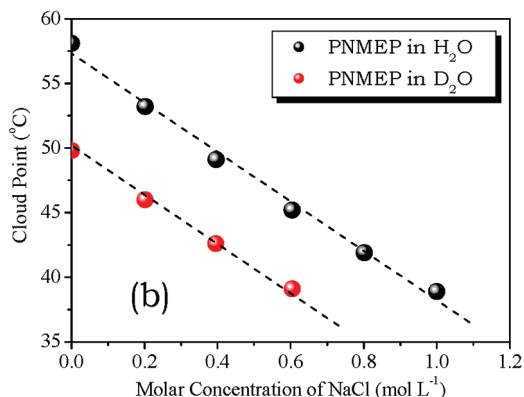
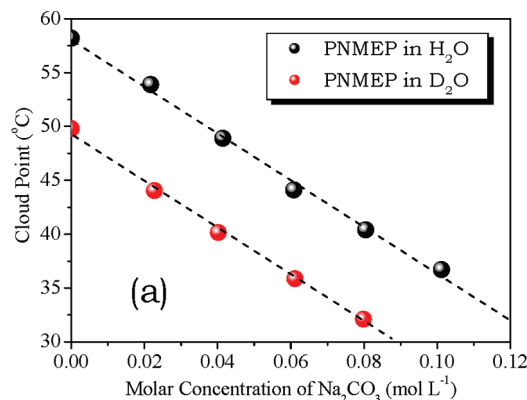


**Figure 13.** Cloud point evolution of a 20.0 mg mL<sup>-1</sup> poly[*N*-(2-methacryloyloxyethyl)pyrrolidone] (PNMEP, <sup>1</sup>H NMR:  $M_n = 47.0$  kg mol<sup>-1</sup>; GPC:  $M_n = 39.0$  kg mol<sup>-1</sup>,  $M_w/M_n = 1.09$ ) solution in D<sub>2</sub>O or H<sub>2</sub>O, as a function of concentration of (a) Na<sub>2</sub>CO<sub>3</sub>, (b) NaCl, or (c) NaI.

methylene protons **d** and **e**, neighboring the amide nitrogen, becomes sharp and narrow. This suggests that iodide anions bind directly to the nitrogen of amide,<sup>57</sup> leading to the significant hydration of its neighboring methylenes.

As shown in Figure 15a, in NaCl solution, the integrals of PNMEP proton signals keep essentially constant below 30 °C. On further elevating the solution temperature, the signal of backbone methyl protons gradually attenuates, followed by the attenuation of signal of spacer methylene protons. The signals of methylene protons neighboring the amide nitrogen of pyrrolidone groups slightly attenuate around the cloud point of 37.7 °C, as assessed by light scattering analysis. This indicates that this temperature-induced dehydration occurs subsequently from polymer backbones, hydrophobic spacers, and finally pyrrolidone groups in NaCl solution.

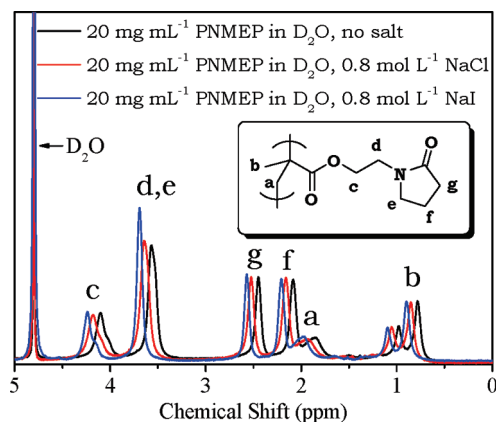


**Figure 14.**  $^1\text{H}$  NMR spectra of a  $20\text{ mg mL}^{-1}$  poly[*N*-(2-methacryloyloxyethyl)pyrrolidone] (PNMEP,  $^1\text{H}$  NMR:  $M_n = 47.0\text{ kg mol}^{-1}$ ; GPC:  $M_n = 39.0\text{ kg mol}^{-1}$ ,  $M_w/M_n = 1.09$ ) solution in  $\text{D}_2\text{O}$  at  $20\text{ }^\circ\text{C}$ ; separately in  $\text{D}_2\text{O}$  absent of salt,  $0.8\text{ mol L}^{-1}$  NaCl solution, or  $0.8\text{ mol L}^{-1}$  NaI solution.

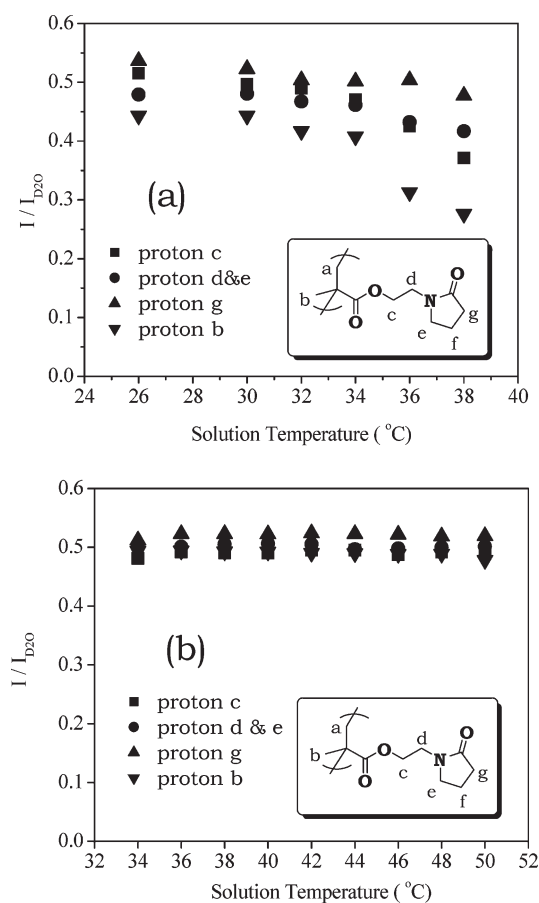


**Figure 15.** Integral ratios of each proton in poly[*N*-(2-methacryloyloxyethyl)pyrrolidone] (PNMEP,  $^1\text{H}$  NMR:  $M_n = 47.0\text{ kg mol}^{-1}$ ; GPC:  $M_n = 39.0\text{ kg mol}^{-1}$ ,  $M_w/M_n = 1.09$ ) to that of  $\text{D}_2\text{O}$  ( $I/I_{\text{D}_2\text{O}}$ ) as a function of solution temperature; (a) in  $0.8\text{ mol L}^{-1}$  NaCl solution, (b) in solution absent of salt.

In contrast, as shown in Figure 15b, in the solution absent of salt, the proton signals of PNMEP do not attenuate around its cloud point of  $49.8\text{ }^\circ\text{C}$ . These results demonstrate that NaCl enhances the hydrophobic association and thus lowers down the cloud point of this polymer. On the other hand, this integral ratio variation is essentially the same as what observed in a long-chain PNMEP

(see Figure 10b). This suggests that the dehydration temperature is higher than the cloud point in solution absent of salt.

## Conclusion

A series of pyrrolidone-based water-soluble polymers, poly[*N*-(2-methacryloyloxyethyl)pyrrolidone] (PNMEP), poly[*N*-(3-acryloyloxypropyl)pyrrolidone] (PNAPP), and poly[*N*-(3-methacryloyloxypropyl)pyrrolidone] (PNMPP), were synthesized via visible light activating RAFT polymerization at  $25\text{ }^\circ\text{C}$ . Kinetic studies indicate a rapid and well-controlled behavior of this RAFT polymerization. Moreover, GPC and  $^1\text{H}$  NMR analysis confirmed the intact molecular structure, well-defined molecular weight, and narrow molecular weight distribution ( $M_w/M_n = 1.08\text{--}1.13$ ) of these polymers.

Laser light scattering measurements demonstrate that the cloud points of these polymers strongly depend on the molecular structure of monomer units. For example, the monomer units of PNMEP and PNAPP have the same elemental composition, but the cloud point of PNMEP at a DP = 96 is  $1.5\text{ }^\circ\text{C}$  lower than that of PNAPP at the same DP = 104. The additional backbone methyl in PNMPP leads to a dramatic cloud point lowering; e.g., PNAPP at a DP = 104 exhibits a cloud point of  $66.5\text{ }^\circ\text{C}$ , while PNMPP at a DP = 100 exhibits a cloud point of  $29.5\text{ }^\circ\text{C}$  in  $\text{H}_2\text{O}$ . This dramatic cloud point lowering is totally contrary to what was observed in PNIPA or PNIPMA.<sup>12</sup> This dramatic cloud point lowering also led Davis and co-workers drawing a conclusion that this polymer was water-insoluble.<sup>50</sup>

This structure character also leads to a dramatic solvent isotopic effect that is contrary to what observed in PNIPA.<sup>60,61</sup> For example, the cloud point of PNMEP at a DP = 237 is  $8.5\text{ }^\circ\text{C}$  lower in  $\text{D}_2\text{O}$  than in  $\text{H}_2\text{O}$ . Increasing the chain length to DP = 415 leads to a  $-8.0\text{ }^\circ\text{C}$  cloud point difference between in  $\text{D}_2\text{O}$  and in  $\text{H}_2\text{O}$ . Increasing the hydrophobicity may suppress this solvent isotopic effect; e.g., for PNMPP at a DP = 100, the cloud point is  $2.8\text{ }^\circ\text{C}$  lower in  $\text{D}_2\text{O}$  than in  $\text{H}_2\text{O}$ .

The cloud points of these pyrrolidone-based polymers are correlated to Hofmeister series. The addition of  $\text{Na}_2\text{CO}_3$  or NaCl leads to the salting-out effect, thereby lowering the cloud point. These salt effect is more pronounced in  $\text{Na}_2\text{CO}_3$  solution, leading to a dramatic decrease of cloud point. However, because  $\text{I}^-$  anions bind directly to the amide nitrogen of pyrrolidone groups, the addition of NaI leads to a salting-in effect, thereby significantly improving the cloud point, up to fully dissolving of PNMEP at  $95\text{ }^\circ\text{C}$ . The solvent isotopic effect in NaCl or  $\text{Na}_2\text{CO}_3$  solution is the same as in solution absent of salt. On the basis of the results of temperature-variable  $^1\text{H}$  NMR and light scattering analysis, upon heating  $\text{D}_2\text{O}$  solution, PNMEP first forms the fully hydrated irregular colloidal aggregates near cloud point, the phase transition occurs at the fully hydrated state at cloud point, and further heating leads to the dehydration and macro-phase separation of this polymer from  $\text{D}_2\text{O}$ . However, in NaCl solution, the dehydration occurs subsequently from polymer backbones, hydrophobic spacers, and finally pyrrolidone groups.

**Acknowledgment.** We thank the National Natural Science Foundation of China (20674064, 20874081) and the Research Fund for Doctoral Program of Higher Education of China (200805300004) for financial support of this research.

**Supporting Information Available:** Figures for  $\text{D}_2\text{O}/\text{H}_2\text{O}$  ratio or salt concentration dependence of light scattering intensity of a  $20.0\text{ mg mL}^{-1}$  PNMEP solution. This material is available free of charge via the Internet at <http://pubs.acs.org>.

## References and Notes

- Roy, D.; Cambre, J. N.; Sumerlin, B. S. *Prog. Polym. Sci.* **2010**, *35*, 278–301.
- Huber, D. L.; Manginell, R. P.; Samara, M. A.; Kim, B.; Bunker, B. C. *Science* **2003**, *301*, 352–354.
- Pasparakis, G.; Cockayne, A.; Alexander, C. J. *J. Am. Chem. Soc.* **2007**, *129*, 11014–11015.
- Akimoto, J.; Nakayama, M.; Sakai, K.; Okano, T. *Biomacromolecules* **2009**, *10*, 1331–1336.
- Wei, H.; Cheng, S.; Zhang, X.; Zhuo, R. *Prog. Polym. Sci.* **2009**, *34*, 893–910.
- Inomata, H.; Goto, S.; Saito, S. *Macromolecules* **1990**, *23*, 4887–4888.
- Gan, L.; Gan, Y.; Deen, G. R. *Macromolecules* **2000**, *33*, 7893–7897.
- Gan, L.; Deen, G. R.; Loh, X. J.; Gan, Y. *Polymer* **2001**, *42*, 65–69.
- Mikheeva, L. M.; Grinberg, N. V.; Mashkevich, A. Y.; Grinberg, V. Y. *Macromolecules* **1997**, *30*, 2693–2699.
- Maeda, Y.; Nakamura, T.; Ikeda, I. *Macromolecules* **2002**, *35*, 217–222.
- Boyko, V.; Richter, S.; Grillo, I.; Geissler, E. *Macromolecules* **2005**, *38*, 5266–5270.
- Tang, Y.; Ding, Y.; Zhang, G. *J. Phys. Chem. B* **2008**, *112*, 8447–8451.
- (a) Cao, Y.; Zhu, X. X.; Luo, J.; Liu, H. *Macromolecules* **2007**, *40*, 6481–6488. (b) Dimitrov, I.; Trzebicka, B.; Muller, A. H. E.; Dworak, A.; Tsvetanov, C. B. *Prog. Polym. Sci.* **2007**, *32*, 1275–1343.
- Lutz, J.-F.; Akdemir, O.; Hoth, A. *J. Am. Chem. Soc.* **2006**, *128*, 13046–13047.
- Lutz, J.-F.; Hoth, A. *Macromolecules* **2006**, *39*, 893–896.
- Lutz, J.-F.; Weichenhan, K.; Akdemir, O.; Hoth, A. *Macromolecules* **2007**, *40*, 2503–2508.
- Einaga, H.; Harada, M. *Langmuir* **2005**, *21*, 2578–2584.
- Tsunoyama, H.; Sakurai, H.; Negishi, Y.; Tsukuda, T. *J. Am. Chem. Soc.* **2005**, *127*, 9374–9375.
- Smith, J. N.; Meadows, J.; Williams, P. A. *Langmuir* **1996**, *12*, 3773–3778.
- Robinson, B. V.; Sullivan, F. M.; Borzelleca, J. F.; Schwartz, S. L. *PVP: A Critical Review of the Kinetics and Toxicology of Polyvinylpyrrolidone (Povidone)*; Lewis Publishers: Chelsea, MI, 1990.
- Xiong, Y.; Cai, H.; Wiley, B. J.; Wang, J.; Kim, M. J.; Xia, Y. *J. Am. Chem. Soc.* **2007**, *129*, 3665–3675.
- Ferrer, D.; Torres-Castro, A.; Gao, X.; Sepúlveda-Guzmán, S.; Ortiz-Méndez, U.; José-Yacamán, M. *Nano Lett.* **2007**, *7*, 1701–1705.
- Hasan, T.; Scardaci, V.; Tan, P.; Rozhin, A. G.; Milne, W. I.; Ferrari, A. C. *J. Phys. Chem. C* **2007**, *111*, 12594–12602.
- O'Connell, M. J.; Bachilo, S. M.; Huffman, C. B.; Moore, V. C.; Strano, M. S.; Haroz, E. H.; Rialon, K. L.; Boul, P. J.; Noon, W. H.; Kittrell, C.; Ma, J.; Hauge, R. H.; Weisman, R. B.; Smalley, R. E. *Science* **2002**, *297*, 593–596.
- Wetzels, G. M. R.; Koole, L. H. *Biomaterials* **1999**, *20*, 1879–1887.
- D'Souza, A. J. M.; Schowen, R. L.; Topp, E. M. *J. Controlled Release* **2004**, *94*, 91–100.
- Le Garrec, D.; Gorb, S.; Luo, L.; Lessard, D.; Smith, D. C.; Yessine, M.-A.; Ranger, M.; Leroux, J.-C. *J. Controlled Release* **2004**, *99*, 83–101.
- Zelikin, A. N.; Such, G. K.; Postma, A.; Caruso, F. *Biomacromolecules* **2007**, *8*, 2950–2953.
- Atobe, I.; Takataf, T.; Endo, T. *Macromolecules* **1994**, *27*, 193–196.
- Iskander, G. M.; Baker, L. E.; Wiley, D. E.; Davis, T. P. *Polymer* **1998**, *39*, 4165–4169.
- He, W.; Gonsalves, K. E.; Pickett, J. H.; Halberstadt, C. *Biomacromolecules* **2003**, *4*, 75–79.
- Gonzalez, N.; Elvira, C.; San Roman, J. *J. Polym. Sci., Polym. Chem.* **2003**, *41*, 395–407.
- Chieffari, J.; Chong, Y. K. B.; Ercole, F.; Krstina, J.; Jeffery, J.; Le, T. P. T.; Mayadunne, R. T. A.; Meijs, G. F.; Moad, C. L.; Moad, G.; Rizzardo, E.; Thang, S. H. *Macromolecules* **1998**, *31*, 5559–5562.
- Lokitz, B. S.; York, A. W.; Stempka, J. E.; Treat, N. D.; Li, Y.; Jarrett, W. L.; McCormick, C. L. *Macromolecules* **2007**, *40*, 6473–6480.
- McCormick, C. L.; Lowe, A. B. *Acc. Chem. Res.* **2004**, *37*, 312–325.
- Li, Y.; Smith, A. E.; Lokitz, B. S.; McCormick, C. L. *Macromolecules* **2007**, *40*, 8524–8526.
- Mertoglu, M.; Laschewsky, A.; Skrabania, K.; Wieland, C. *Macromolecules* **2005**, *38*, 3601–3614.
- Laschewsky, A.; Mertoglu, M.; Kubowicz, S.; Thünemann, A. F. *Macromolecules* **2006**, *39*, 9337–9345.
- McCullough, L. A.; Dufour, B.; Tang, C.; Zhang, R.; Kowalewski, T.; Matyjaszewski, K. *Macromolecules* **2007**, *40*, 7745–7747.
- Schilli, C. M.; Zhang, M.; Rizzardo, E.; Thang, S. H.; Chong, Y. K.; Edwards, K.; Karlsson, G.; Müller, A. H. E. *Macromolecules* **2004**, *37*, 7861–7866.
- Li, Y.; Lokitz, B. S.; Armes, S. P.; McCormick, C. L. *Macromolecules* **2006**, *39*, 2726–2728.
- Zhang, J.; Jiang, X.; Zhang, Y.; Li, Y.; Liu, S. *Macromolecules* **2007**, *40*, 9125–9132.
- Walther, A.; Millard, P.; Goldmann, A.; Lovestead, T.; Schacher, F.; Barner-Kowollik, C.; Müller, A. H. E. *Macromolecules* **2008**, *41*, 8608–8619.
- Smith, A. E.; Xu, X.; McCormick, C. L. *Prog. Polym. Sci.* **2010**, *35*, 45–93.
- Lu, L.; Yang, N.; Cai, Y. *Chem. Commun.* **2005**, 5287–5288.
- Lu, L.; Zhang, H.; Yang, N.; Cai, Y. *Macromolecules* **2006**, *39*, 3770–3776.
- Jiang, W.; Lu, L.; Cai, Y. *Macromol. Rapid Commun.* **2007**, *28*, 725–728.
- Shi, Y.; Gao, H.; Lu, L.; Cai, Y. *Chem. Commun.* **2009**, 1368–1370.
- Shi, Y.; Liu, G.; Gao, H.; Lu, L.; Cai, Y. *Macromolecules* **2009**, *42*, 3917–3926.
- Deng, J.; Shi, Y.; Jiang, W.; Peng, Y.; Lu, L.; Cai, Y. *Macromolecules* **2008**, *41*, 3007–3014.
- Convertine, A. J.; Lokitz, B. S.; Lowe, A. B.; Scales, C. W.; Myrick, L. J.; McCormick, C. L. *Macromol. Rapid Commun.* **2005**, *26*, 791–795.
- Benaglia, M.; Rizzardo, E.; Alberti, A.; Guerra, M. *Macromolecules* **2005**, *38*, 3129–3140.
- McLeary, J. B.; McKenzie, J. M.; Tonge, M. P.; Sanderson, R. D.; Klumperman, B. *Chem. Commun.* **2004**, 1950–1951.
- McLeary, J. B.; Calitz, F. M.; McKenzie, J. M.; Tonge, M. P.; Sanderson, R. D.; Klumperman, B. *Macromolecules* **2004**, *37*, 2383–2394.
- Xia, Y.; Yin, X.; Burke, N. A. D.; Stöver, H. D. H. *Macromolecules* **2005**, *38*, 5937–5943.
- Furyk, S.; Zhang, Y.; Ortiz-Acosta, D.; Cremer, P. S.; Bergbreiter, D. E. *J. Polym. Sci., Polym. Chem.* **2006**, *44*, 1492–1501.
- Zhang, Y.; Furyk, S.; Bergbreiter, D. E.; Cremer, P. S. *J. Am. Chem. Soc.* **2005**, *127*, 14505–14510.
- Zhang, Y.; Furyk, S.; Sagle, L. B.; Cho, Y.; Bergbreiter, D. E.; Cremer, P. S. *J. Phys. Chem. C* **2007**, *111*, 8916–8924.
- Cho, Y.; Sagle, L. B.; Imura, S.; Zhang, Y.; Kherb, J.; Chilkoti, A.; Scholtz, J. M.; Cremer, P. S. *J. Am. Chem. Soc.* **2009**, *131*, 15188–15193.
- Kujawa, P.; Winnik, F. M. *Macromolecules* **2001**, *34*, 4130–4135.
- Mao, H.; Li, C.; Zhang, Y.; Furyk, S.; Cremer, P. S.; Bergbreiter, D. E. *Macromolecules* **2004**, *37*, 1031–1036.
- Nemethy, G.; Scheraga, H. A. *J. Chem. Phys.* **1964**, *41*, 680–689.
- Sun, B.; Lin, Y.; Wu, P.; Siesler, H. W. *Macromolecules* **2008**, *41*, 1512–1520.
- Wang, X.; Wu, C. *Macromolecules* **1999**, *32*, 4299–4301.
- Schild, H. G.; Tirrell, D. A. *J. Phys. Chem.* **1990**, *94*, 4352–4356.
- Suwa, K.; Freitag, R.; Garret-Flaudy, F. *Langmuir* **2002**, *18*, 3434–3440.
- Hofmeister, F. *Arch. Exp. Pathol. Pharmacol.* **1888**, *24*, 247–260.
- Mao, H. B.; Li, C. M.; Zhang, Y. J.; Bergbreiter, D. E.; Cremer, P. S. *J. Am. Chem. Soc.* **2003**, *125*, 2850–2851.
- Zhang, Y.; Mao, H.; Cremer, P. S. *J. Am. Chem. Soc.* **2003**, *125*, 15630–15635.
- Mao, H.; Li, C.; Zhang, Y.; Furyk, S.; Cremer, P. S.; Bergbreiter, D. E. *Macromolecules* **2004**, *37*, 1031–1036.